RESEARCH PAPER

Antitumour activity of ANG1005, a conjugate between paclitaxel and the new brain delivery vector Angiopep-2

A Régina[1], M Demeule[2], C Ché[2], I Lavallée[2], J Poirier[1], R Gabathuler[2], R Béliveau[1] and J-P Castaigne[2]

[1]Laboratoire de Médecine Moléculaire, Chemistry Department, Université du Québec à Montréal, Montréal, Québec, Canada and [2]Angiochem, Research Department, Montreal, Québec, Canada

Background and purpose: Paclitaxel is highly efficacious in the treatment of breast, head and neck, non-small cell lung cancers and ovarian carcinoma. For malignant gliomas, paclitaxel is prevented from reaching its target by the presence of the efflux pump P-glycoprotein (P-gp) at the blood–brain barrier. We investigated the utilization of a new drug delivery system to increase brain delivery of paclitaxel.
Experimental approach: Paclitaxel molecules were conjugated to a brain peptide vector, Angiopep-2, to provide a paclitaxel–Angiopep-2 conjugate named ANG1005. We determined the brain uptake capacity, intracellular effects and antitumour properties of ANG1005 in vitro against human tumour cell lines and in vivo in human xenografts. We then determined ANG1005 activity on brain tumours with intracerebral human tumour models in nude mice.
Key results: We show by in situ brain perfusion that ANG1005 enters the brain to a greater extent than paclitaxel and bypasses the P-gp. ANG1005 has an antineoplastic potency similar to that of paclitaxel against human cancer cell lines. We also demonstrate that ANG1005 caused a more potent inhibition of human tumour xenografts than paclitaxel. Finally, ANG1005 administration led to a significant increase in the survival of mice with intracerebral implantation of U87 MG glioblastoma cells or NCI-H460 lung carcinoma cells.
Conclusions and implications: These results demonstrate the antitumour potential of a new drug, ANG1005, and establish that conjugation of anticancer agents with the Angiopep-2 peptide vector could increase their efficacy in the treatment of brain cancer.
British Journal of Pharmacology advance online publication, 23 June 2008; doi:10.1038/bjp.2008.260

Introduction

Treatment of brain cancer remains one of the biggest challenges in oncology. Anaplastic astrocytomas (grade III) and glioblastomas (grade IV) are the most aggressive brain tumours with median survival of patients of 24 and 9 months, respectively (Kemper et al., 2004). Aggressiveness is due to their rapid proliferation, high angiogenic level and tendency to infiltrate the surrounding healthy tissue (Louis, 2006). Surgery, external beam radiation therapy and systemic chemotherapy prolong the median survival span of patients for only 4 months (Chang et al., 2006). The low efficiency of currently available systemic chemotherapy for brain tumour treatments is in part due to the presence of the

blood–brain barrier (BBB) that separates the blood from the cerebral parenchyma and restricts the penetration of most drugs into the CNS (Deeken and Loscher, 2007).

Paclitaxel, a diterpene natural product, isolated from the yew tree *Taxus brevifolia* (Wani et al., 1971), is one of the most active cancer chemotherapeutic agents known. It acts by promoting microtubule assembly and stabilizes microtubule dynamics, preventing them from depolymerizing, leading to inhibition of cell proliferation and induction of apoptosis (Foa et al., 1994; Gupta et al., 2003). It is commonly used to treat ovarian, breast and non-small cell lung cancer (Crown and O'Leary, 2000; McGrogan et al., 2007). *In vitro*, paclitaxel has been shown to be active against gliomas and brain metastases (Cahan et al., 1994; Tseng et al., 1999). However, in patients with recurrent primary brain tumours, paclitaxel has shown only modest activity (Chamberlain and Kormanik, 1995). Lack of uptake of

Correspondence: Dr R Gabathuler, Angiochem, 201 President-Kennedy Ave, Suite PK-R220, Montreal, Québec, Canada H2X 3Y7.
E-mail: rgabathuler@angiochem.com

paclitaxel by brain is associated with low BBB permeability due to the expression of the multidrug resistance efflux pump P-glycoprotein (P-gp) at the apical membrane of the brain endothelial cells (Breedveld *et al.*, 2006). Expression of P-gp limits the entry of paclitaxel both in normal brain and also in brain tumours where the blood capillaries are thought to be 'leaky'. Different strategies to increase paclitaxel delivery to the brain have been investigated, from invasive drug-releasing implants to drug delivering nanoparticles (Nikanjam *et al.*, 2007; Tanner *et al.*, 2007).

Several approaches have been described for drug delivery to the brain, such as local invasive delivery by direct injection or infusion, induction of enhanced permeability as well as various physiological targeting strategies (Begley, 2004; Gaillard *et al.*, 2005; Pardridge, 2007). We have identified a new family of peptides, named Angiopeps, as a new brain drug delivery system for pharmacological agents that do not readily enter the brain (Demeule *et al.*, 2008). The very efficient transport of these peptides into the brain is the main property for their use as vectors to transport drugs across the BBB. Angiopep-2, a 19-amino-acid peptide, was one of the vectors designed to target the low-density lipoprotein receptor-related protein to mediate transcytosis across the BBB.

The aim of the present study was to investigate the potential of this brain delivery platform to serve as a paclitaxel delivery system to treat recurrent primary or metastatic brain tumours. We synthesized a paclitaxel–Angiopep-2 conjugate, named ANG1005. We demonstrated that ANG1005 crosses the BBB and distributes into the brain parenchyma at a much higher level than free paclitaxel. We also demonstrated that ANG1005 exerts cytotoxic effects on tumour cell lines comparable to that of free paclitaxel, and acts as free paclitaxel at the G2–M-phase junction and induces microtubule stabilization in tumour cells. In addition, we assessed its efficiency to overcome the P-gp using mdr1a-deficient mice. We investigated the *in vivo* antitumour efficacy of ANG1005 and found that treatments with ANG1005 were highly effective in brain and lung carcinoma tumour xenograft models and resulted in significant increased mice survival in orthotopic brain tumour model in nude mice. Overall, our results show that ANG1005, a paclitaxel–peptide conjugate, represents a new drug with good potential for the treatment of primary or metastatic brain tumours.

Methods

Animals
All animals used in these studies were handled and maintained in accordance with the Guidelines of the Canadian Council on Animal Care (CCAC). Animal protocols were approved by the Institutional Animal Care and Use Committee of Université du Québec à Montréal.

Animals were obtained from Charles River Laboratories Inc. (Saint-Constant, QC, Canada) and were allowed to acclimatize for 5 days before experiments. Brain perfusion studies were performed on adult male Crl: CD-1 mice (25–30 g, 6–8 weeks old) (Charles River Canada, St-Constant, QC, Canada)

and adult female CF-1 mice (mdr1a $(+/+)$ and $(-/-)$, 30–40 g, 6–8 weeks old) (Charles River Inc, Wilmington, MA). Female athymic nude mice (Crl:Nu/Nu-*nu*BR) (20–25 g, 4–6 weeks old) (Charles River Canada, St-Constant, QC, Canada) were used for tumour models and were maintained in a pathogen-free environment.

ANG1005 synthesis
Angiopep-2 peptide has three potential sites for conjugation to 2′-*N*-succinimide-paclitaxel (2′-NHS-paclitaxel). Paclitaxel molecules were conjugated to Angiopep-2 using a cleavable ester linkage. Briefly, for the preparation of the paclitaxel–Angiopep-2 conjugate, 1 mol equivalent of Angiopep-2 was directly added to a solution of 2′-NHS-paclitaxel. The reaction was performed in 68% dimethyl sulphoxide (DMSO) in Ringer's solution, pH 7.2 for about 24 h at 12 °C. Reaction was followed by HPLC. During the reaction, Angiopep-2 and 2′-NHS-paclitaxel peaks disappeared mainly to yield a major product. This major product was purified by hydrophobic chromatography, analysed and sequenced by mass spectrometry. Analysis showed that the product formed was a paclitaxel–Angiopep-2 conjugate, with three paclitaxel molecules attached to one Angiopep-2 molecule. This conjugate was selected and named ANG1005.

HPLC conditions
HPLC analysis were performed using the SCL-10A HPLC system (Shimadzu Scientific Instruments, Columbia, MD, USA) with DGU-14A degasser unit, LC-10AT binary pump, SIL-10AF auto injector and CTO-10AS thermostated column compartment. Chromatographic separations were carried out using a TAXSIL column (4.6 mm × 50 mm, 3 μm particle size; Varian, Palo Alto, CA, USA) at a flow rate of 1.0 mL min^{-1} and a constant temperature of 23 °C. Mobile phase consisted of a mixture of acetonitrile (ACN)–trifluoroacetic acid 0.05% and water–trifluoroacetic acid 0.05% as a mobile phase. Quantitative detection was carried out using a photodiode array detector SPD-M10A (Shimadzu Scientific Instruments) at a detection wavelength of 229 nm. Data were acquired and processed using chromatography manager software Class VP (7.2.1 SP1) from Shimadzu. The chromatographic conditions used for analysis were equilibration (0.25 min, 30:70 ACN/water), isocratic gradient (2 min, 30:70 ACN/water), linear gradient (until 7 min, 65:35 ACN/water), isocratic gradient (until 12 min, 65:35 ACN/water), linear gradient (12.13 min, 30:70 ACN/water) and re-equilibration (until 15 min, 30:70 ACN/water).

Iodination of ANG1005
ANG1005 was radiolabelled using the iodo-beads kit from Pierce (Rockford, IL, USA). Briefly, beads were washed twice with 3 mL of phosphate-buffered saline (PBS) on a Whatman filter and resuspended in 60 μL of PEG-400 (100%, pH = 6.6). Na^{125}I (1 mCi) was added to the bead suspension for 5 min at room temperature. Iodination of ANG1005 was initiated by addition of 1 mg of ANG1005 diluted in 100 μL of DMSO–Ringer's HEPES (80:20) for 15 min. [^{125}I]ANG1005 was then

purified by hydrophobic chromatography using a column pre-packed with 30 RPC resin (GE Healthcare, Baie d'Urfé, QC, Canada) to remove free iodine. Purified radiolabelled ANG1005 was then analysed by HPLC and C18 column.

[³H]ANG1005 synthesis

Paclitaxel (9 mg, 10.5 μmol) was spiked with 1 mCi of [³H]paclitaxel (4.8 Ci mmol⁻¹). The mixture was used for the synthesis of [³H]ANG1005 according to the procedure described above. After the conjugation step, 50 μCi of [³H]ANG1005 was recovered with a specific activity of $0.14 \, \mu Ci \, nmol^{-1}$.

In situ *mouse brain perfusion*

The transport of [¹²⁵I]ANG1005 and [³H]paclitaxel in mouse brain was measured using the *in situ* brain perfusion method adapted in our laboratory for the study of drug uptake in the mouse brain (Dagenais et al., 2000; Demeule et al., 2002). In situ brain perfusion of [¹⁴C]inulin in the presence of unlabelled ANG1005 was also performed to verify the physical integrity of the BBB. Briefly, the right common carotid of mice anaesthetized with ketamine/xylazine (140/8 mg kg⁻¹, i.p.) was exposed and ligated at the level of the bifurcation of the common carotid, rostral to the occipital artery. The common carotid artery was then catheterized rostrally with polyethylene tubing filled with heparin (25 U mL⁻¹) and mounted on a 26-gauge needle. The syringe containing the perfusion fluid ([¹²⁵I]ANG1005, [³H]paclitaxel, [¹⁴C]inulin at the appropriate concentrations in Krebs/bicarbonate buffer (128 mM NaCl, 24 mM NaHCO₃, 4.2 mM KCl, 2.4 mM NaH₂PO₄, 1.5 mM CaCl₂, 0.9 mM MgCl₂ and 9 mM D-glucose) gassed with 95% O₂ and 5% CO₂ to obtain a pH of 7.4, and warmed to 37 °C in a water bath) was placed in an infusion pump (Harvard pump PHD 2000; Harvard Apparatus, Saint-Laurent, QC, Canada) and connected to the catheter. Prior to the perfusion, the contralateral blood flow contribution was eliminated by severing heart ventricles. The brain was perfused for 5 min at a flow rate of 1.15 mL min⁻¹. After perfusion, the brain was further perfused for 60 s with Krebs buffer, to wash out the excess of radiolabelled molecules. Mice were then decapitated to terminate perfusion and the right hemisphere was quickly isolated on ice before being subjected to capillary depletion. Briefly, for capillary depletion, the mice brain was homogenized on ice in Ringer's HEPES buffer with 0.1% BSA in a glass homogenizer. Brain homogenate was then mixed thoroughly with 35% Dextran 70 (50:50) and centrifuged at 5400 g for 10 min at 4 °C. The supernatant composed of brain parenchyma and the pellet representing capillaries were then carefully separated. Aliquots of homogenates, supernatants, pellets and perfusates were taken to measure their contents in radiolabelled molecules. Aliquots of the perfusion fluid were also collected and weighed to determine tracer concentrations in the perfusate. [¹²⁵I]ANG1005 samples were counted in a Wizard 1470 Automatic Gamma Counter (Perkin-Elmer Inc., Woodbridge, ON, USA). [³H]paclitaxel and [¹⁴C]inulin samples were digested in 2 mL of Solvable (Packard) at 50 °C and mixed with 9 mL of Ultima gold XR scintillation cocktail (Packard). Radioactivity was counted in a Packard Tri-carb model 1900 TR.

Drug accumulation studies

Cellular uptake of [³H]paclitaxel and [³H]ANG1005 was measured in P-gp-overexpressing MDCK-MDR1 cells, grown in 24-well plates. Cells were washed three times with PBS and preincubated for 30 min at 37 °C in culture medium without serum with or without the P-gp inhibitor cyclosporin A (10 μM). Radiolabelled molecules (50 nM) were then added for 60 min. The cells were rapidly washed three times with ice-cold PBS and then lysed in 500 μL of 0.1 M NaOH. The amount of radiolabelled molecules retained in the cells was counted by β-scintillation counting (Packard model 1900 TR). An aliquot of cell lysate was used in parallel to determine cellular protein concentration.

In vitro *cytotoxicity assay*

For the thymidine uptake assay, tumour cells were cultured in 96-well plates at a density of 5000 cells per well. After incubation of cells with paclitaxel or ANG1005 for 48 h, the medium was aspirated, and cells were pulse labelled for 2 h at 37 °C with a medium containing 2 μCi mL⁻¹ [methyl-³H]thymidine (GE Healthcare). Cells were harvested and placed in a MicroBeta counter (1450 MicroBeta Liquid scintillation and Luminescence Counter; Perkin-Elmer) for determination of tritium uptake. As a control, ANG1005 was incubated in medium with serum for 48 h at 37 °C. Stability of the molecule was estimated by HPLC after ACN extraction.

Immunofluorescence of tubulin

NCI-H460 cells were grown on 24-well plates for 2–3 days in culture medium. Cells were then treated for 24 h, with paclitaxel (30 nM), or ANG1005 (10 nM). Thereafter, cells were fixed and permeabilized with cold methanol for 10 min at –20 °C. After blocking with 2% BSA in phosphate buffer (PBS), fixed cells were incubated with anti-β-tubulin monoclonal antibody (CP07; Calbiochem, Mississauga, ON, USA) for 1 h in PBS–0.1% BSA. After three washes, fluorescein isothiocyanate-conjugated anti-mouse IgG rabbit antibody (Jackson Immunoresearch, Westgrove, PA, USA) was added into each well. Pictures of cells were taken at × 400 using a Qimaging RETIRA 1300 camera attached to a Nikon fluorescence microscope (Nikon Eclipse TE2000-U) with Northern Eclipse software.

In vitro *cell cycle analysis using flow cytometry*

U87 MG cells in exponential growth in 25 cm² flasks were treated with equimolar concentrations of ANG1005 (30 nM) or paclitaxel (100 nM) for 24 h. After treatment, attached cells were released by trypsinization. Cells were centrifuged, washed twice with PBS and fixed with 70% ice-cold ethanol. Fixed cells were resuspended in a DNA staining solution containing 50 μg mL⁻¹ propidium iodide (Sigma-Aldrich, Oakville, ON, USA), 0.5 mg mL⁻¹ RNAse, in 10 mM Tris and 5 mM MgCl₂. DNA cellular content was analysed by

fluorescence-activated cell sorting with a FACS Calibur flow cytometer (Becton Dickinson, San Jose, CA, USA) using CellQuest Pro software, version 4.0.2.

Tumour implantation, evaluation and treatments

Tumour xenografts were established by subcutaneous inoculation of 2.5×10^6 U87 cells or NCI-H460 cells, suspended in 100 μL of serum-free cell culture medium in the right flank of CD-1 nude mice under light isoflurane anaesthesia (Rolland *et al.*, 2007). Palpable tumours developed typically within 7–10 days. On the day of first treatment, mice bearing a 100–200 mm^3 subcutaneous tumour were pooled and randomly assigned to control and treated groups of 4–6 animals. Animals with tumour outside the desired volume range were excluded. Tumour size and body weight of the animals were measured daily by the same investigator. For tumour growth kinetics, two-dimensional measurements were taken with an electronic caliper and tumour volume was calculated according to the following formula: tumour volume $(mm^3) = \pi/6 \times length \times width^2$.

Intracerebral tumour models were established by stereotactic inoculation of 5×10^5 U87 cells or NCI-H460 cells in mice. At 1 h before surgery, mice received a subcutaneous injection of buprenorphine (0.1 mg kg^{-1}). For tumour cell inoculation, mice were anaesthetized by injection of ketamine/xylazine (120/10 mg kg^{-1}, i.p.) and placed in a stereotactic apparatus (Kopf, Tujunga, CA, USA). A burr hole was drilled 1.5 mm anterior and 2.5 mm lateral to the bregma. The cell suspension in 5 μL of serum-free cell culture medium was injected over a 5-min period, using a Hamilton syringe at a depth of 3.5 mm. Drug treatments were started 3 days post-tumour cell inoculation. Clinical signs of disease progression and body weights were monitored everyday. When mice reached terminal end points they were killed by carbon dioxide inhalation.

Administration of the treatments

Paclitaxel was given intravenously by bolus tail-vein injection, daily for five consecutive days. Paclitaxel solution (6 mg mL^{-1}) was prepared in EtOH/Cremophor (1/1, v/v) and further diluted (1:3, v/v) with sterile saline (0.85% NaCl). Injection solution was prepared freshly before every injection to nude mice. ANG1005 was given intravenously by bolus tail-vein or by intraperitoneal injection. ANG1005 formulation was prepared in Solutol/Ringer's HEPES (25/75, v/v). Solutol HS15, a non-ionic surfactant, was used as a solubilizer for ANG1005. ANG1005 powder was vortexed in pre-heated Solutol (65 °C), pre-heated (65 °C) Ringer's HEPES was added and the suspension was heated by microwave (5–10 cycles of 10 s) until complete solubilization. After the solubilization procedure, the formulation was analysed on HPLC to verify the purity and stability of ANG1005 in its formulation.

Evaluation of drug efficacy

Effect of drug treatments on xenograft tumour growth was evaluated when the first mouse from the control group had a tumour reaching 1000 mm^3. Difference with tumour volumes at the day of first treatment was calculated at this time point and tumour growth inhibition of treated groups versus control was estimated. For intracerebral tumour models, the life-prolonging effect of treatments was evaluated by determination of the median survival time (MST days) after tumour inoculation for each group from the Kaplan–Meier plot using GraphPad Prism software (GraphPad Software, San Diego, CA, USA). The increase in the life span (ILS%) was calculated as $((TMST/CMST) - 1) \times 100$, where T_{MST} and C_{MST} are the MST of the drug-treated mice and the vehicle-treated mice, respectively.

Statistical analysis

All values reported are expressed as means ± s.d. All statistical analyses were performed using GraphPad Prism version 4.0 °C for Macintosh (GraphPad Software). Statistical analyses were performed using Student's *t*-test when one group was compared with the control group. To compare two or more groups with the control group, one-way ANOVA with Dunnett's *post hoc* test was used. Significance was assumed for *P*-values less than 0.05.

Cell lines and reagents

Paclitaxel was purchased from InB:Paxis Pharmaceuticals (Boulder, CO, USA). Angiopep-2 peptide was synthesized by Peptidec (Pierrefonds, QC, Canada) and also by Peptisyntha (Torrance, CA, USA). Iodo-beads were purchased from Sigma-Aldrich. Tumour cell lines (U87 MG, NCI-H460, U118, U251, A549, Calu-3 and SK-OV-3) were purchased from American Type Culture Collection (ATCC) (Manassass, VA, USA). Na^{125}I and [^{14}C]inulin were purchased from Amersham-Pharmacia Biotech (Baie d'Urfé, QC, Canada). [^{3}H]Paclitaxel was purchased from American Radiolabeled Chemicals (St Louis, MO, USA). Solutol HS 15 (poly-oxyethylene esters of 12-hydroxystearic acid) was purchased from BASF Pharma Solutions (Mississauga, ON, USA). Other biochemical reagents were purchased from Sigma-Aldrich. P-gp-overexpressing MDCK-MDR1 cells (MDCK cells transduced with the cDNA for human MDR1) were a gift from Dr Amanda Yancy from AstraZeneca Pharmaceuticals LP (Wilmington, DE, USA).

Results

Synthesis and chemical structure of ANG1005

The structure of the paclitaxel–Angiopep-2 conjugate named ANG1005 is defined as [N-(2′succinyl-paclitaxel)Thr]-Phe-Phe-Tyr-Gly-Gly-Ser-Arg-Gly-[N-(2′succinyl-paclitaxel)Lys]-Arg-Asn-Asn-Phe-[N-(2′succinyl-paclitaxel)Lys]-Thr-Glu-Glu-Tyr. The chemical structure of ANG1005 conjugate is shown in Figure 1a. Each ANG1005 molecule consists of three paclitaxel molecules attached to one Angiopep-2 molecule by cleavable ester linkages. A scheme of the ANG1005 synthetic pathway is shown in Figure 1b. Paclitaxel was first activated by conversion into 2′-NHS-paclitaxel in two steps. In the conjugation step (step 3), amines (amino-terminal and lysines in positions 10 and 15) in Angiopep-2 peptide react with 2′-NHS-paclitaxel. A molecular weight of 5109.14 g mol^{-1} was defined by mass spectrometry confirming that three paclitaxel molecules are conjugated to one Angiopep-2 peptide.
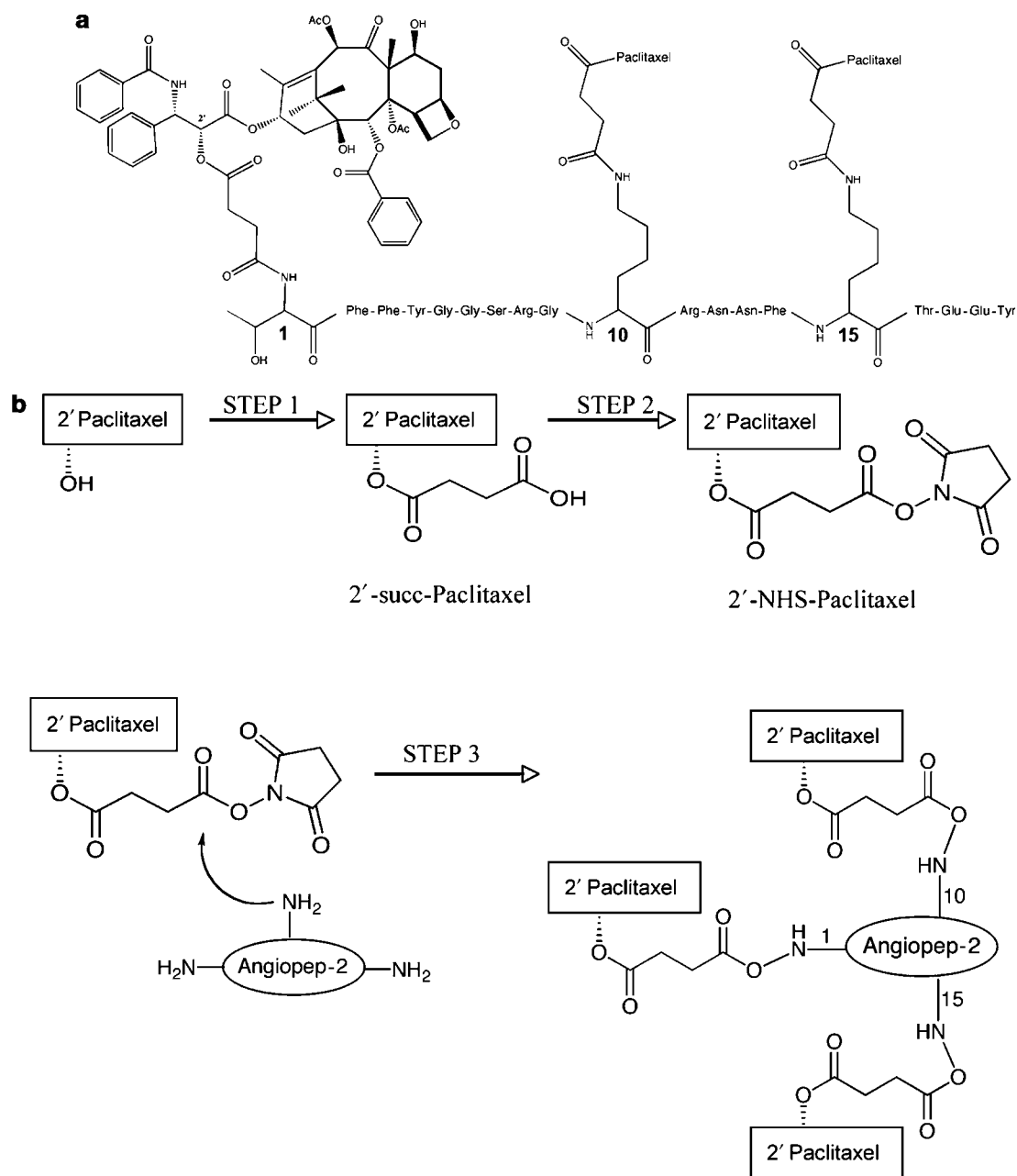
Figure 1 Chemical structure and synthetic scheme for ANG1005. (**a**) ANG1005 is composed of three molecules of paclitaxel linked by a cleavable succinyl ester linkage to the Angiopep-2 peptide. (**b**) Schematic representation of ANG1005 synthesis steps. Paclitaxel was first activated by conversion into N-succinimide (2'-NHS)-paclitaxel in two steps. In the conjugation step (step 3), amines (amino-terminal and lysines in positions 10 and 15) in the Angiopep-2 peptide react with 2'-NHS-paclitaxel.

Chromatographic separation and iodination of ANG1005

Figure 2a shows representative peaks obtained with the same HPLC method. Angiopep-2, paclitaxel and ANG1005 were seen to elute at three clearly distinct retention times with RT = 2.0, 6.6 and 7.2 min for Angiopep-2, paclitaxel and ANG1005, respectively. ANG1005 was radiolabelled by iodination and [^{125}I]ANG1005 was purified by reverse phase using 30 RPC resin to remove excess of free [^{125}I]. Radiolabelled ANG1005 was then analysed by HPLC on a C18 column, monitoring effluent at 229 nm. Fractions were collected and measured for radioactivity. Figure 2b shows that the [^{125}I]ANG1005 peak was not affected by the

radiolabelling procedure. No other peak was detected by HPLC analysis. Furthermore, 98% of the radioactivity was found to be associated with the ultraviolet peak of ANG1005.

Brain uptake of ANG1005 conjugate

To evaluate the brain distribution of the ANG1005 conjugate, we measured its brain uptake by *in situ* mouse brain perfusion and compared it to the brain uptake of free paclitaxel. Mouse brains were perfused for 5 min with [^{125}I]ANG1005 or [^{3}H]paclitaxel. After perfusion with the tracers, the brain was further perfused for 60 s with Ringer's
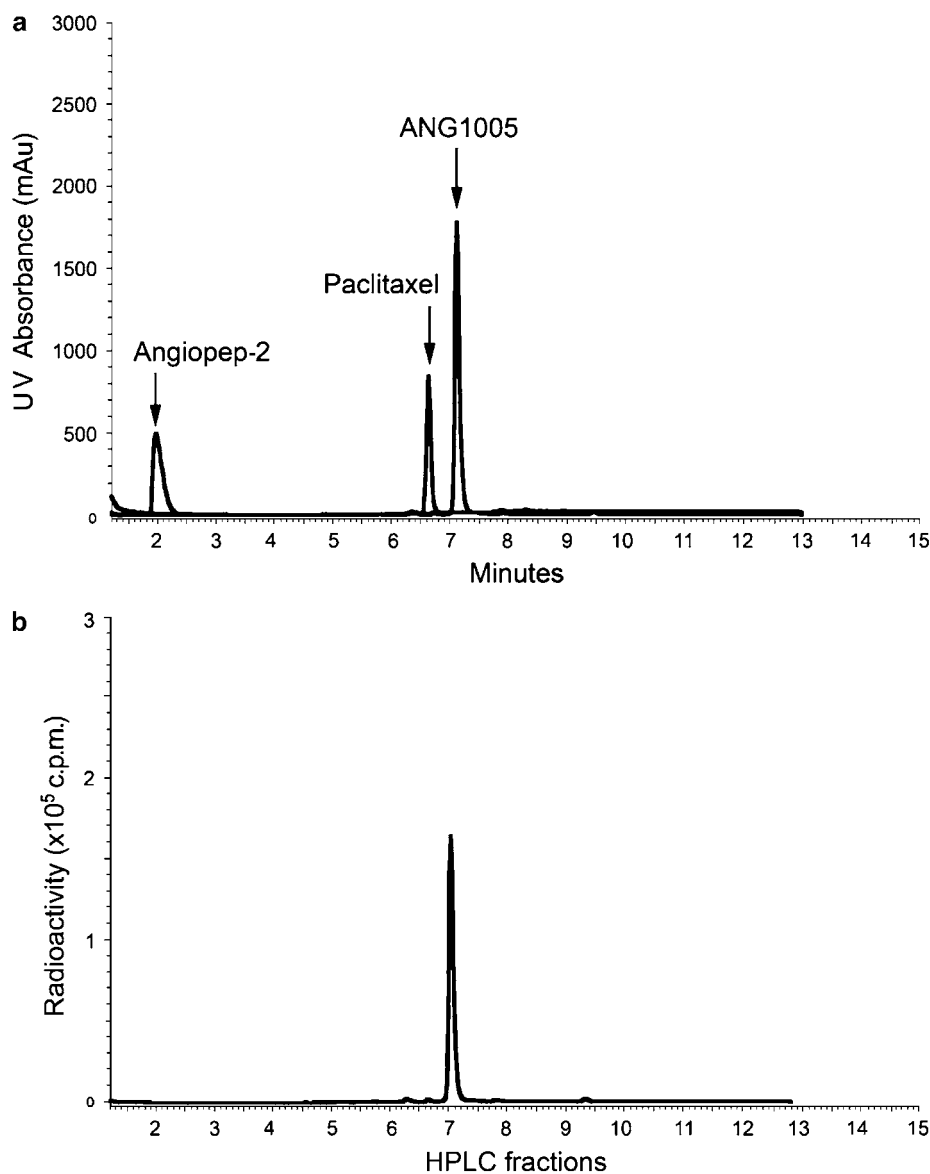
Figure 2 HPLC analysis of Angiopep-2, paclitaxel, ANG1005 and [^{125}I]ANG1005. (**a**) Representative chromatograms obtained for Angiopep-2, paclitaxel and ANG1005 using the same HPLC method, showing three distinct retention times. (**b**) HPLC analysis of [^{125}I]ANG1005. After the radiolabelling and purification of the labelled ANG1005 on 30 RPC resin, HPLC analysis was performed at a flow rate of 1 mL min^{-1} to evaluate the incorporation of ^{125}I on ANG1005. Fractions of 1 mL were collected and the radioactivity associated with these fractions was quantified in a gamma counter.

solution to wash out the excess of radiolabelled molecules. The right brain hemisphere was isolated on ice and capillary depletion was performed. Aliquots of homogenates, supernatants, pellets and perfusates were taken to measure their contents in radiolabelled molecules. Figure 3a shows that the total brain uptake of ANG1005 conjugate was 4.5-fold higher than that of free paclitaxel. Furthermore, considering that there are three molecules of paclitaxel in every molecule of ANG1005, the potential increase in paclitaxel brain uptake is even higher. The volume of distribution of inulin was assessed in the presence of unlabelled ANG1005. The addition of ANG1005 did not affect the volume of distribution of inulin (data not shown), indicating that the BBB integrity was unaffected by the ANG1005. Furthermore, to demonstrate the specificity of the ANG1005 brain uptake

mechanism, *in situ* brain perfusion was performed in the presence of an excess of unconjugated Angiopep-2. Mouse brains were perfused for 1 min with 10 nM [^{125}I]ANG1005 in the presence or absence of 100 nM Angiopep-2. Figure 3b shows that ANG1005 brain uptake was significantly inhibited, by 25%, in the presence of unlabelled Angiopep-2.

In situ *brain perfusion of paclitaxel and ANG1005 in* mdr1a-deficient *and control mice*

To evaluate the interaction between ANG1005 and the efflux pump P-gp, we then compared the brain parenchyma uptake of [^{3}H]paclitaxel and [^{125}I]ANG1005 conjugate by *in situ* brain perfusion in mdr1a-deficient and control mice. Mouse brain was perfused for 5 min with radiolabelled molecules.
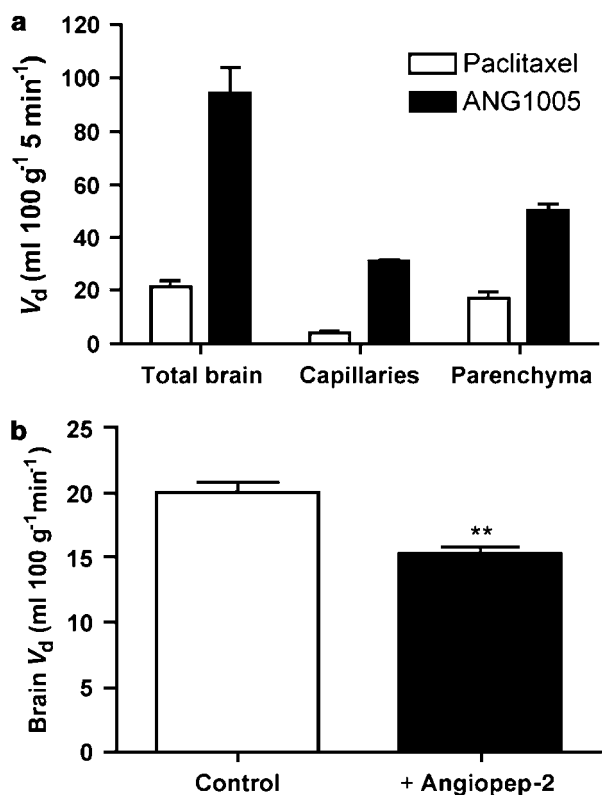
Figure 3 Brain uptake of ANG1005 measured by *in situ* brain perfusion. In (a), CD-1 mice were perfused with 50 nM of [^{125}I]ANG1005 or 50 nM of [^{3}H]paclitaxel for 5 min as described in the Methods section. After perfusion, brain capillary depletion was performed on the mice right brain hemispheres. The amount of radioactivity associated with total brain homogenate, the brain capillary fraction and with the parenchyma was evaluated. The results were expressed as the apparent volume of distribution (V_d) for the radiolabelled drugs found in these brain compartments. Data represent the means ± s.d. obtained for at least three mice. In (b), the inhibition of ANG1005 brain uptake by unconjugated Angiopep-2 was measured. CD-1 mice were perfused with 10 nM of [^{125}I]ANG1005 for 1 min in the presence or absence of Angiopep-2 (100 nM). The amount of radioactivity associated with total brain homogenate was evaluated. The results were expressed as the apparent volume of distribution (V_d) for the radiolabelled ANG1005 found in the brain homogenate. Data represent the means ± s.d. obtained from three mice for each group (**$P<0.01$).

After perfusion, the brain was further perfused for 60 s with Ringer's solution to wash out the excess of radiolabelled molecules. The right brain hemisphere was isolated on ice before being subjected to capillary depletion. Figure 4a shows that the brain parenchyma uptake of [^{3}H]paclitaxel was increased by 2.2-fold in mdr1a(−/−) compared to wild-type mice. By contrast, no difference was found in the brain parenchyma uptake of [^{125}I]ANG1005 between mdr1a(−/−) and wild-type mice. The absence of interaction between P-gp and ANG1005 was further evaluated using a conjugate synthetized with [^{3}H]paclitaxel. [^{3}H]-Paclitaxel–Angiopep-2 conjugate was synthetized following the same protocol as ANG1005. Uptake of [^{3}H]paclitaxel and [^{3}H]paclitaxel–Angiopep-2 (3:1) conjugate ([^{3}H]ANG1005) was monitored in P-gp-overexpressing MDCK-MDR cells in the presence or absence of the P-gp modulator cyclosporin A. Figure 4b shows that [^{3}H]paclitaxel uptake was significantly increased
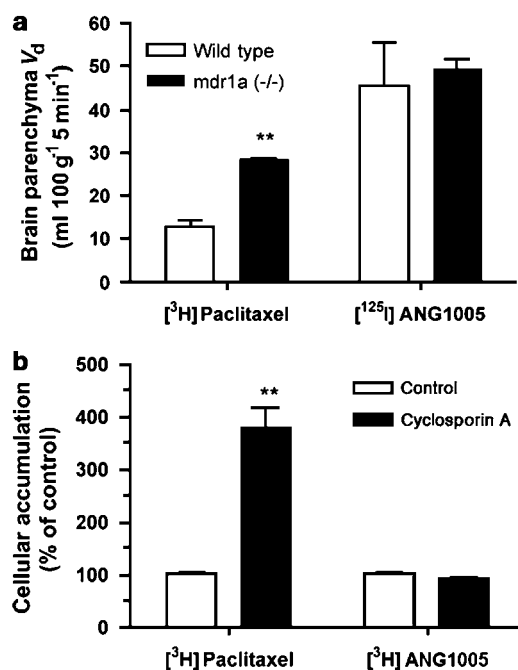

Figure 4 Lack of interaction between P-gp and ANG1005 in brain uptake. (a) Brain parenchyma uptake of paclitaxel and ANG1005 measured by *in situ* brain perfusion in wild-type and mdr1a-deficient mice. Mice were perfused with 50 nM of [^{125}I]ANG1005 or 50 nM of [^{3}H]paclitaxel for 5 min as described in the Methods section. After perfusion, brain capillary depletion was performed on the mice right brain hemispheres. The amount of radioactivity associated with total brain homogenate, the brain capillary fraction and with the parenchyma was evaluated. The results were expressed as the apparent volume of distribution (V_d) for the radiolabelled drugs found in the brain parenchyma. Data represent the means ± s.d. obtained for at least three mice. (b) Effects of the P-gp modulator, cyclosporin A, on [^{3}H]paclitaxel and [^{3}H]ANG1005 accumulation in MDCK-MDR cells. Cells were preincubated for 30 min at 37 °C in culture medium alone (control) or culture medium containing 10 μM cyclosporin A. Then 50 nM of radiolabelled molecules were added and cellular accumulation was measured after incubation for 1 h. Data are means ± s.e.m. (bars) values expressed as percentage of control, obtained from three independent experiments ($n=6$) (**$P<0.01$).

by more than threefold in the presence of cyclosporin A, whereas no difference was observed for [^{3}H]ANG1005.

In vitro *cytotoxic activity of ANG1005 and paclitaxel*
The *in vitro* cytotoxic activity of ANG1005 against human tumour cell lines was evaluated and compared to that of paclitaxel, using the thymidine incorporation assay. Tumour cells were incubated for 48 h in the presence of increasing concentrations of ANG1005 or paclitaxel. Tumour cells were then incubated in the presence of [^{3}H]thymidine for 2 h at 37 °C and [^{3}H]thymidine incorporation was then evaluated in a beta counter. Results presented in Table 1 show that ANG1005 conjugate exhibits high cytotoxicity with IC$_{50}$ values ranging from 2.7 to 8.3 nM. ANG1005 showed activity comparable to that of paclitaxel in glioblastoma, lung carcinoma and ovarian carcinoma cell lines.

Effect of ANG1005 on tubulin polymerization
Paclitaxel acts by blocking cell cycle progression during mitosis by binding and stabilizing microtubules. We

investigated whether the ANG1005 conjugate behaved similarly. NCI-H460 cells were treated for 24 h at equimolar concentrations of paclitaxel (30 nM) or ANG1005 (100 nM), then fixed and stained with anti-tubulin antibody. Figure 5a shows the morphological changes after 24 h treatment with cell shrinkage observed with either drug treatment. Figure 5b shows tubulin detection using immunofluorescence. A well-defined flat structure of a tubulin network is observed in the cytoplasm of control untreated cells, whereas treatments at equimolar doses of paclitaxel or ANG1005 induce the formation of microtubule bundles in the cytoplasm of numerous cells.

Table 1 *In vitro* cytotoxicity of ANG1005 and paclitaxel

Cell line	IC_{50} (nM)	
	ANG1005	*Paclitaxel*
Glioblastoma		
U87 MG	5.1	6.4
U118	2.7	7.2
U251	4.5	9.3
Lung carcinoma		
NCI-H460	5.2	7.3
A549	2.9	3.6
Calu-3	8.3	17.2
Ovarian carcinoma		
SK-OV-3	3.1	4.9

Human cancer cells were exposed to increasing concentrations of ANG1005 or paclitaxel as described in the Methods section. Incorporation of [^{3}H]thymidine was measured as a function of drug concentrations. The drug concentrations required to inhibit cell proliferation by 50% (IC_{50}) were calculated. Results are mean of 3–5 experiments ($n = 8$).

Cell cycle analysis

We also performed fluorescence-activated cell sorting analysis on U87 cells incubated with equimolar concentrations of ANG1005 or paclitaxel for 24 h to investigate intracellular effect of ANG1005. Cells were stained with propidium iodide and analysed for DNA content. As shown in Figure 6, both drugs caused an arrest at the G_2/M phase of the cell cycle in the U87 MG tumour cells. Analysis of the cell percentage in each phase indicated that after 24 h 19% of control cells were in G_2/M phase compared to 68 and 52% in paclitaxel and ANG1005-treated cells, respectively.

Antitumour effect of ANG1005 on human tumour xenografts in nude mice

As a first step to evaluate ANG1005 *in vivo* antitumoral activity, experiments were performed to determine whether the ANG1005 conjugate could affect the growth of human tumour xenografts in athymic nude mice. NCI-H460 non-small cell lung carcinoma cells were implanted subcutaneously into female nude mice. Treatments started 8 days after implantation when tumours had reached a volume of 100–150 mm³. Before each treatment, stability of formulated ANG1005 was verified by HPLC analysis. Figure 7 shows a representative chromatogram of ANG1005 in the Solutol/Ringer's HEPES formulation compared to ANG1005 solubilized in 100% DMSO. ANG1005 stability was unaffected by the formulation procedure and only trace amount of free paclitaxel was present in the administered ANG1005 formulation. In this study, treatments were administered to compare the two drugs using the same administration schedule and dose level. Control group received vehicle (Solutol 25%), treated groups received paclitaxel (10 mg kg⁻¹) or ANG1005 (20 mg kg⁻¹) every third day for a total of five injections. As
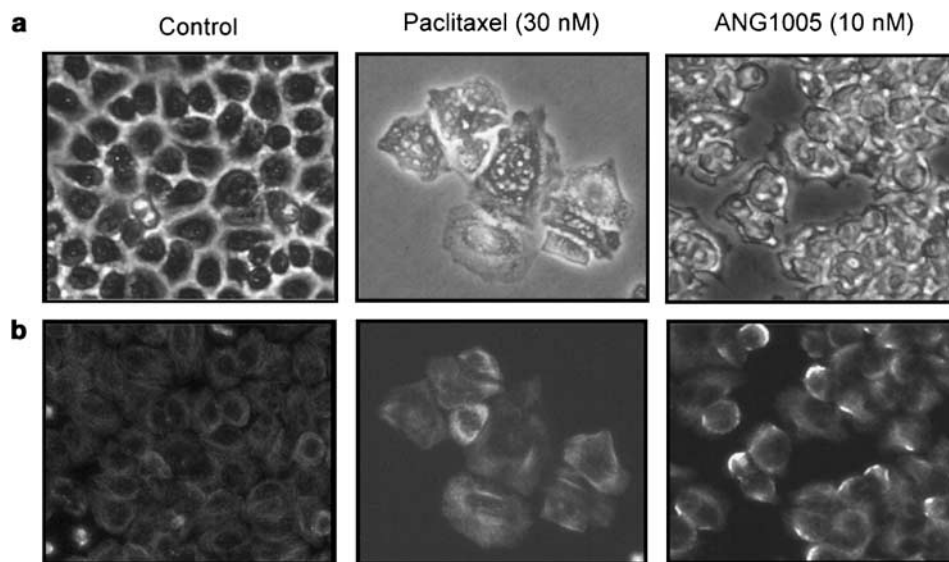

Figure 5 Morphological changes and immunofluorescence of tubulin. (**a**) NCI-H460 cells (2.5×10^4) were pre-cultured for 48 h on 24-well plates and then treated with paclitaxel (30 nM) or ANG1005 (10 nM) for 24 h. Cell morphology was observed and photographed after treatment ($\times 400$). (**b**) Tubulin detection was performed as described in the Methods section. Briefly, fixed cells were reacted with anti-β-tubulin monoclonal antibody for 1 h followed by reaction with fluorescein isothiocyanate-conjugated anti-mouse IgG rabbit antibody added into each well. Pictures of cells were taken ($\times 400$) with a Qimaging RETIRA 1300 camera attached to a Nikon fluorescence microscope (Nikon Eclipse TE2000-U).

approximately half the molecular weight of ANG1005 is contributed by three molecules of paclitaxel, a $20 \, mg \, kg^{-1}$ dose of ANG1005 is roughly equivalent to $10 \, mg \, kg^{-1}$ of paclitaxel. Figure 8a shows tumour growth of control versus treated groups. At 19 days after tumour inoculation, tumours from paclitaxel and ANG1005 groups have average volumes of 483 and $236 \, mm^3$, respectively, compared to $845 \, mm^3$ in the control group. Corresponding tumour growth inhibition was thus higher in ANG1005-treated group (82.8%) than in paclitaxel-treated group (48.6%).

In the second type of study, U87 MG glioblastoma cells were implanted subcutaneously into female nude mice. Treatments were administered to compare the two drugs at their maximum tolerated dose. Treated mice received 0, $40 \, mg \, kg^{-1}$ (daily $\times 5$ then twice weekly) of ANG1005 by intraperitoneal injection or $20 \, mg \, kg^{-1}$ (daily $\times 5$) of paclitaxel by intravenous injection, starting at 12 days post-subcutaneous implantation. Preliminary blood pharmacokinetic studies were performed and showed that contrary to paclitaxel, ANG1005 presents a similar bioavailability after i.v. or i.p. bolus injection (data not shown). On the basis of these results, dosage of ANG1005 could be increased with i.p. bolus injections. As shown in Figure 8b, both paclitaxel and ANG1005 treatments resulted in a marked reduction in tumour size compared to pretreatment. At 22 days after the first treatment day, tumours from paclitaxel and ANG1005 groups had average volumes of 91 and $159 \, mm^3$, respectively compared to 206 and $194 \, mm^3$ on the first day of treatment. Corresponding tumour growth inhibition was thus similar in ANG1005-treated group (107%) and in paclitaxel-treated group (122%). The body weights of the mice were unaffected by all treatments and none of the mice that received either paclitaxel or ANG1005 conjugate died because of the treatments (data not shown).
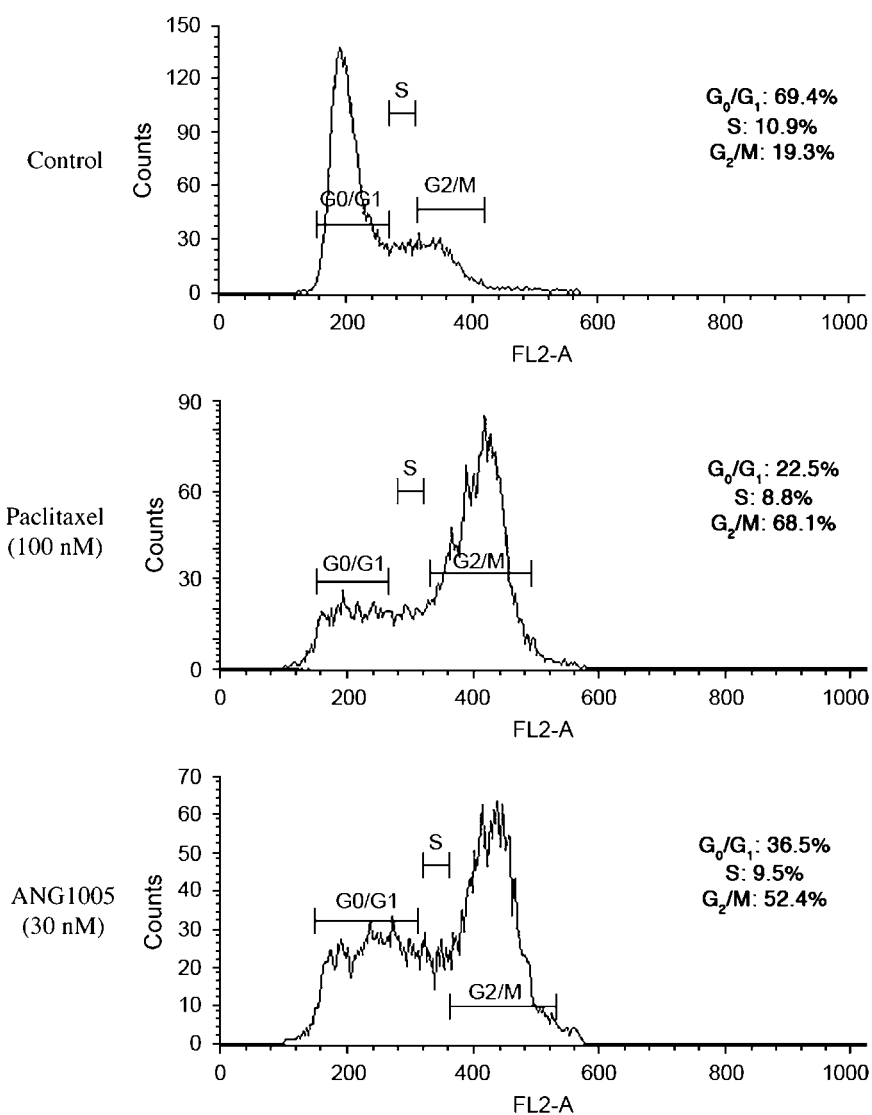

Figure 6 Paclitaxel and ANG1005 effects on cell cycle. U87 MG glioblastoma cells were treated with equimolar concentrations of ANG1005 (30 nM) or paclitaxel (100 nM) for 24 h. Cell cycle analysis was performed as described in the Methods section. Briefly, fixed cells were resuspended in a propidium iodide DNA staining solution. DNA cellular content was analysed with a FACS Calibur flow cytometer and CellQuest Pro Software (Becton Dickinson, San Jose, CA, USA). One representative experiment out of three is shown.

Effect of ANG1005 on mice survival

Intracerebral tumour models were used to evaluate the potential activity of ANG1005 on brain tumours. U87 MG glioblastoma cells were implanted by stereotaxy in nude mice brains and survival was determined. At 3 days after implantation, animals were treated by intraperitoneal injection with vehicle only (control group) or with ANG1005 ($50\,mg\,kg^{-1}$). Treatments were then administered twice a week until animals were killed. Mice were monitored every day for clinical symptoms and weight loss. They were killed when they reached terminal clinical end points. As shown in Figure 9a, animals receiving ANG1005 treatment showed improved survival compared with controls. The calculated MST of ANG1005-treated and vehicle-treated groups is presented in Table 2. Statistical analysis indicated that ANG1005 treatment prolonged the MST of mice with an increase in life span of 15% ($P<0.05$).

Effect of ANG1005 on a brain xenograft lung tumour model was also evaluated. NCI-H460 non-small cell lung carcinoma cells were intracerebrally implanted in nude mice. At 3 days after cell implantation, mice were treated by intraperitoneal injection with vehicle only (control group) or with increasing dose of ANG1005 (20 and $50\,mg\,kg^{-1}$). As shown in Figure 9b, animals receiving ANG1005 treatment showed improved survival compared with controls. As presented in Table 2, this effect was dose dependent as the median survival for the control group was 11 days, whereas the MST for mice receiving 20 and $50\,mg\,kg^{-1}$ were 13 and 14 days, respectively. Statistical analysis indicated that the MST of mice receiving 20 or $50\,mg\,kg^{-1}$ of ANG1005 was significantly prolonged.

Discussion

In the present study, we investigated the potential of a new approach to deliver paclitaxel to the brain for the treatment of primary and metastatic brain tumours. A new chemical entity paclitaxel–Angiopep-2 has been synthetized. This new drug, ANG1005, combines a receptor-targeting peptide vector to the brain (Angiopep-2) with three molecules of paclitaxel. *In vivo* brain perfusion and *in vitro* studies indicated that ANG1005 has a higher brain uptake than paclitaxel and bypasses P-gp at the BBB. *In vitro* studies have demonstrated that ANG1005 maintains numerous mechanisms comparable to paclitaxel with inhibition of tumour cell proliferation, blockage of tumour cells in G2/M phase and induction of β-tubulin polymerization. Furthermore, *in vivo* activity studies performed with tumour xenografts showed that ANG1005 presents a high activity against tumour growth. Efficacy studies in brain tumour models (orthotopic and metastatic) showed that ANG1005 treatment significantly increased mice survival.

Despite its high hydrophobicity, we found by *in situ* brain perfusion in mice that paclitaxel brain uptake is relatively low ($0.69\pm0.25\,\mu L\,g^{-1}\,s^{-1}$) in accordance with values found in the literature (K_{in} paclitaxel $= 0.53\pm0.2\,\mu L\,g^{-1}\,s^{-1}$) (Blanc *et al.*, 2004). We found that ANG1005 brain uptake exceeds paclitaxel brain uptake by 4- to 5-fold. ANG1005 is composed of three paclitaxel molecules, thus in molar terms, the total potential increase in paclitaxel accumulation may represent 12- to 15-fold. Capillary depletion was performed to distinguish between the fraction remaining in the endothelial cells and the drug that had crossed the abluminal side of endothelial cells to enter the brain parenchyma. More than 65% of ANG1005 was found associated with brain parenchyma. Invasive therapy using paclitaxel for brain tumours such as intra-tumour convention-enhanced delivery has shown a high antitumour response rate and also a high incidence of treatment-associated severe side effects (Lidar *et al.*, 2004; Tanner *et al.*, 2007). Nanoparticles loaded with paclitaxel have also been evaluated for paclitaxel chemotherapy across the BBB (Feng *et al.*, 2004; Koziara *et al.*, 2004; Nikanjam *et al.*, 2007) and the entrapment of
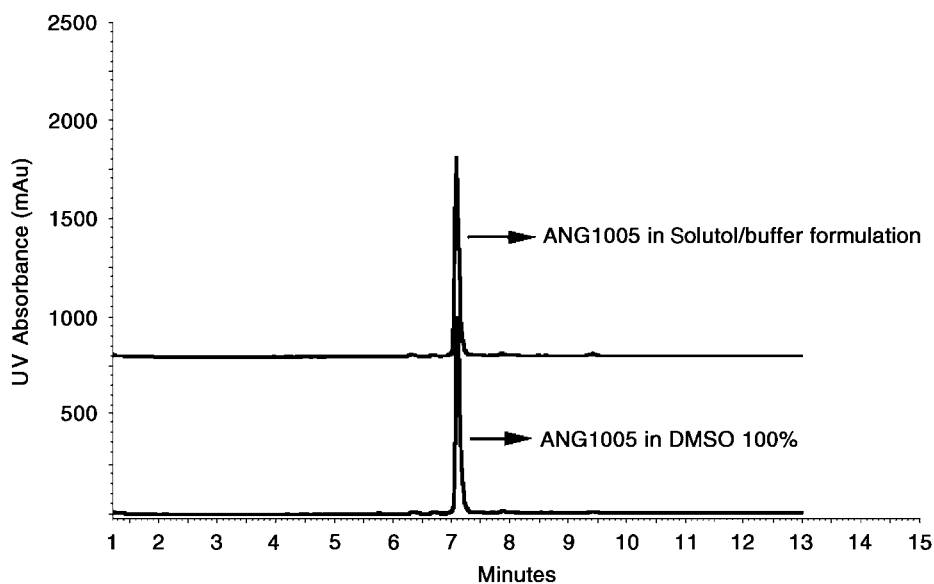
Figure 7 HPLC analysis of ANG1005 in formulation. Representative chromatograms of ANG1005 solubilized in dimethyl sulphoxide (DMSO) 100% and ANG1005 in Solutol/Ringer's HEPES buffer formulation. ANG1005 was solubilized in DMSO 100% or formulated as described in the Methods section. Both preparations were analysed by HPLC.
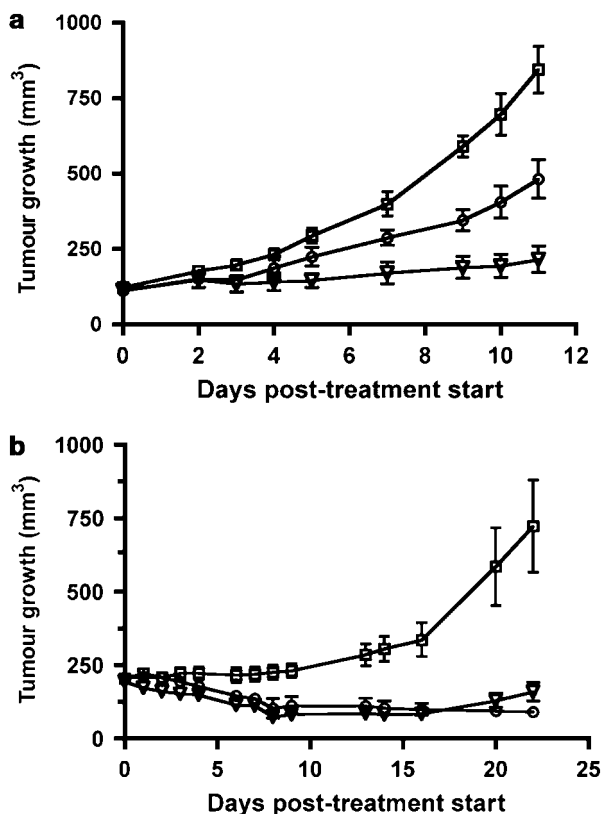
Figure 8 Antitumour activity of paclitaxel and ANG1005 against U87 MG glioblastoma and NCI-H460 lung carcinoma xenografts. (**a**) Tumour growth curves of NCI-H460 non-small cell lung carcinoma xenografts. NCI-H460 non-small cell lung carcinoma cells were subcutaneously implanted in the right flank of female nude mice. Treatments started on day 8 when tumour volumes reached 100–125 mm^3; intravenous paclitaxel (10 mg kg^{-1}, every third day, for five doses), intravenous ANG1005 (20 mg kg^{-1}, every third day, for five doses). (**b**) Tumour growth curves of U87 MG glioblastoma xenografts. U87 glioblastoma cells were subcutaneously implanted in the right flank of nude mice. Treatments started on day 12 when tumour volume reached 250–300 mm^3; intravenous paclitaxel (20 mg kg^{-1}, once a day for 5 days), intraperitoneal ANG1005 (40 mg kg^{-1}, once a day for 5 days and then 100 mg kg^{-1} every third day, for two doses). Experiment was repeated separately at least three times. One representative experiment is shown out of five.

paclitaxel in nanoparticles significantly increased the drug brain uptake. However, the application of nanoparticles has been the subject of controversy due to potential nonspecific opening of the BBB (Olivier *et al.*, 1999; Lockman *et al.*, 2004). We have demonstrated previously that the Angiopep family transcytosis across the brain endothelium did not involve BBB opening (Demeule *et al.*, 2008).

The expression and activity of P-gp is the major factor that limits the use of paclitaxel for the treatment of brain tumours (Fellner *et al.*, 2002; Geney *et al.*, 2002). Different attempts have been made to circumvent or diminish the interaction between paclitaxel and P-gp at the BBB by chemical modification of the paclitaxel molecule (Cisternino *et al.*, 2003; Rice *et al.*, 2005). We investigated the influence of the P-gp-mediated efflux across the BBB on the accumulation of paclitaxel and ANG1005 in the brain. We used P-gp knockout (mdr1a-deficient) mice that provide a direct indication of the impact of P-gp expression on the brain

disposition of drugs (Schinkel *et al.*, 1995). Brain parenchyma uptake of paclitaxel was enhanced by 2.2-fold in mdr1a knockout mice compared to wild-type mice. This corresponds to previously reported increase in normal brain and brain tumour of paclitaxel concentration in P-gp knockout mice (Gallo *et al.*, 2003). Interestingly, this study had shown that even in brain tumours where the BBB is considered leaky, P-gp remains a limiting factor to paclitaxel entry. By contrast, the brain parenchyma uptake of ANG1005 was the same in both P-gp knockout and wild-type mice. The same absence of interaction was demonstrated in P-gp-overexpressing MDCK-MDR1 cells, using a conjugate with tritiated paclitaxel and Angiopep-2, demonstrating that the entire conjugate bypasses the P-gp. This strongly indicates that contrary to paclitaxel, the expression of P-gp does not influence ANG1005 entry into the brain. It had been shown for chemotherapeutic drugs, such as doxorubicin and paclitaxel, that conjugation with a brain delivery peptide allowed P-gp bypass at the BBB level (Rousselle *et al.*, 2000; Blanc *et al.*, 2004). In our study, the uptake of ANG1005 into the brain parenchyma of mdr1a-deficient mice was higher than the uptake of paclitaxel showing that the non-interaction with P-gp is not the only factor to explain the difference in brain uptake of the two molecules. Studies have shown that co-administration of paclitaxel with P-gp modulators led to increase in brain paclitaxel levels and increased activity against paclitaxel-sensitive brain tumours, but also toxic side effects resulting from increased drug levels due to P-gp modulation in peripheral tissues (Fellner *et al.*, 2002). ANG1005 may provide a safer way to increase paclitaxel brain level and thus the therapeutic effects against brain tumours, with fewer toxic effects in the periphery.

The *in vitro* potency of paclitaxel on brain tumour cells from different species origin has been well demonstrated (Cahan *et al.*, 1994). We found that ANG1005 is also highly cytotoxic against a large panel of human tumour cell lines, including glioblastoma cell lines, with IC$_{50}$ values in the same range as those previously reported for paclitaxel. Thus, the chemical conjugation did not affect paclitaxel's high *in vitro* potency. ANG1005 stability experiments performed in culture medium at 37 °C showed that there was no release of free paclitaxel in the culture medium after 48 h. These results show that the cytotoxicity of ANG1005 is not due to an extracellular liberation of free paclitaxel but is mediated by membrane translocation of the intact conjugate. Paclitaxel binding to the β-subunit of tubulin promotes the assembly of stable microtubules and inhibits the disassembly process, thus interfering with the G2 and M phases of the cell cycle (Crown and O'Leary, 2000). We demonstrate that ANG1005 treatment affects microtubule polymerization and provokes the characteristic accumulation of cells in G2/M phase. Thus, ANG1005 presents the same primary cellular activity as paclitaxel. The proposed mechanism of action for ANG1005 in tumour cells is an intracellular release of paclitaxel by esterase cleavage and subsequent action on tubulin, the intracellular target of paclitaxel.

Paclitaxel is highly potent against various tumour xenografts (Rose, 1992). We showed that ANG1005 is also highly cytotoxic *in vivo* as it inhibited the growth of
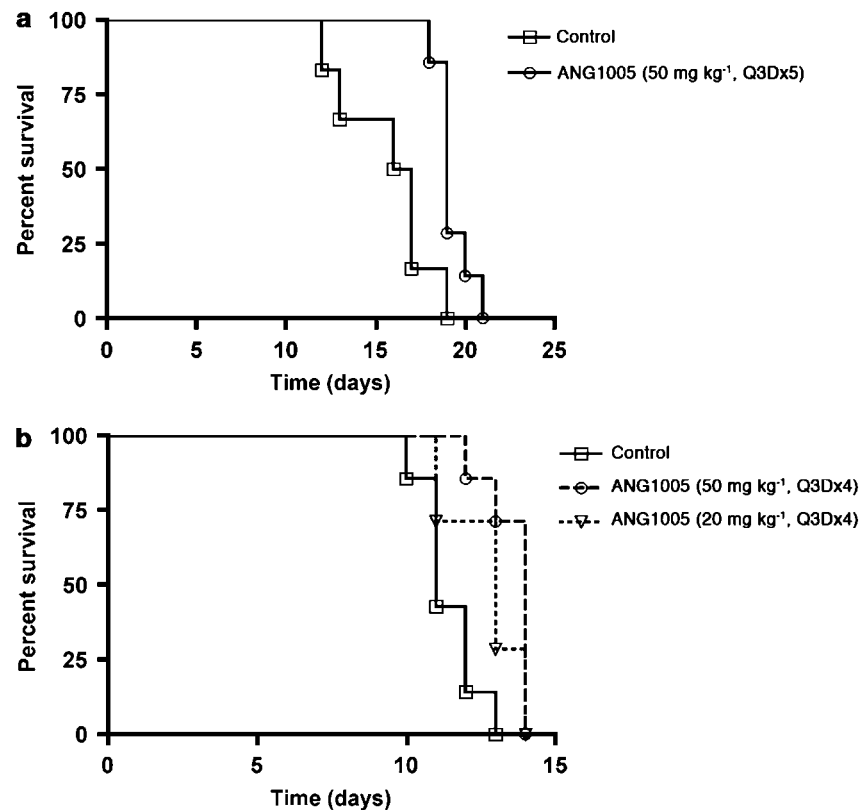
Figure 9 Percentage of survival (Kaplan–Meier plot) of mice with intracerebral U87 MG glioblastoma and NCI-H460 lung carcinoma tumours. (**a**) Nude mice received intracerebral implantation of U87 MG cells. At 3 days post-implantation, animals were treated by intravenous injection with vehicle only (control group) or ANG1005 ($50 \, mg \, kg^{-1}$, every third day, for five doses). (**b**) Nude mice received intracerebral implantation of NCI-H460 lung carcinoma cells. At 3 days post-implantation, animals were treated with vehicle only (control group) or ANG1005 (20, $50 \, mg \, kg^{-1}$, every third day, for four doses). The experiment was repeated separately at least three times. One representative experiment is shown ($n = 6$).

Table 2 ANG1005 effects on survival of mice with intracerebral tumours

Tumour	ANG1005 ($mg \, kg^{-1}$)	MST (days)	ILS (%)	P-values
Glioblastoma				
	0	16.5	0	
	50	19	15	0.02
Lung carcinoma				
	0	11	0	
	20	13	18	0.002
	50	14	27	0.002

Abbreviations: ILS, increase in life span; MST, median survival time.
Values shown are from groups of 4–6 mice, with or without treatment with ANG1005 in the doses shown. The statistical significance of the effects of ANG1005 on ILS was assessed from the Kaplan–Meier plot; the relevant *P*-values are shown.

xenografts U87 MG glioblastoma as well as NCI-H460 lung carcinoma. Vehicle toxicity limited the dosing and impeded the evaluation of a higher drug concentration effect. Whereas the systemic concentration of paclitaxel after an i.p. injection is insignificant (Gelderblom *et al.*, 2002), ANG1005 treatment was efficacious after an i.p. injection. Paclitaxel is highly efficacious for cancers outside the brain, its efficacy against cancers inside the brain is very low (Chamberlain and Kormanik, 1995, 1999). The potential

activity of ANG1005 against brain tumours was assessed with intracerebral tumour models. Importantly, ANG1005 administration prolonged survival of mice bearing intracranial U87 MG glioblastoma and NCI-H460 lung carcinoma tumours. Conjugation of chemotherapeutic drugs with brain delivery peptides had previously been performed (Rousselle *et al.*, 2000; Jones and Shusta, 2007) showing that the conjugates were capable of crossing the BBB at higher levels than the free drugs. More specifically, paclitaxel has been conjugated with the cell delivery vector penetratin (pAntp) (Wang *et al.*, 2006). This conjugate showed a good antitumour activity *in vitro*. However, *in vivo* antitumoral activity was not reported in those studies. We demonstrate here that the new drug ANG1005 is active in brain tumour models *in vivo*. This is a critical step showing that the Angiopep-2 brain peptide vector approach represents an efficient therapeutic strategy for increasing the potency of anticancer agents for brain tumours. ANG1005 has recently entered in phase I clinical trials in patients with recurrent primary or secondary metastatic brain tumours.

Conflict of interest

M Demeule, C Ché, I Lavallée, R Gabathuler and J-P Castaigne are employed by Angiochem.

References

Begley DJ (2004). ABC transporters and the blood–brain barrier. *Curr Pharm Des* **10**: 1295–1312.

Blanc E, Bonnafous C, Merida P, Cisternino S, Clair P, Scherrmann JM *et al.* (2004). Peptide-vector strategy bypasses P-glycoprotein efflux, and enhances brain transport and solubility of paclitaxel. *Anticancer Drugs* **15**: 947–954.

Breedveld P, Beijnen JH, Schellens JH (2006). Use of P-glycoprotein and BCRP inhibitors to improve oral bioavailability and CNS penetration of anticancer drugs. *Trends Pharmacol Sci* **27**: 17–24.

Cahan MA, Walter KA, Colvin OM, Brem H (1994). Cytotoxicity of taxol *in vitro* against human and rat malignant brain tumors. *Cancer Chemother Pharmacol* **33**: 441–444.

Chamberlain MC, Kormanik P (1995). Salvage chemotherapy with paclitaxel for recurrent primary brain tumors. *J Clin Oncol* **13**: 2066–2071.

Chamberlain MC, Kormanik P (1999). Salvage chemotherapy with taxol for recurrent anaplastic astrocytomas. *J Neurooncol* **43**: 71–78.

Chang SM, Butowski NA, Sneed PK, Garner IV (2006). Standard treatment and experimental targeted drug therapy for recurrent glioblastoma multiforme. *Neurosurg Focus* **20**: E4.

Cisternino S, Bourasset F, Archimbaud Y, Semiond D, Sanderink G, Scherrmann JM (2003). Nonlinear accumulation in the brain of the new taxoid TXD258 following saturation of P-glycoprotein at the blood–brain barrier in mice and rats. *Br J Pharmacol* **138**: 1367–1375.

Crown J, O'Leary M (2000). The taxanes: an update. *Lancet* **355**: 1176–1178.

Dagenais C, Rousselle C, Pollack GM, Scherrmann JM (2000). Development of an *in situ* mouse brain perfusion model and its application to mdr1a P-glycoprotein-deficient mice. *J Cereb Blood Flow Metab* **20**: 381–386.

Deeken JF, Loscher W (2007). The blood–brain barrier and cancer: transporters, treatment, and Trojan horses. *Clin Cancer Res* **13**: 1663–1674.

Demeule M, Poirier J, Jodoin J, Bertrand Y, Desrosiers RR, Dagenais C *et al.* (2002). High transcytosis of melanotransferrin (P97) across the blood–brain barrier. *J Neurochem* **83**: 924–933.

Demeule M, Regina A, Che C, Poirier J, Nguyen T, Gabathuler R *et al.* (2008). Identification and design of new peptides as a drug delivery system for the brain. *J Pharmacol Exp Ther* **324**: 1064–1072.

Fellner S, Bauer B, Miller DS, Schaffrik M, Fankhanel M, Spruss T *et al.* (2002). Transport of paclitaxel (Taxol) across the blood–brain barrier *in vitro* and *in vivo*. *J Clin Invest* **110**: 1309–1318.

Feng SS, Mu L, Win KY, Huang G (2004). Nanoparticles of biodegradable polymers for clinical administration of paclitaxel. *Curr Med Chem* **11**: 413–424.

Foa R, Norton L, Seidman AD (1994). Taxol (paclitaxel): a novel antimicrotubule agent with remarkable anti-neoplastic activity. *Int J Clin Lab Res* **24**: 6–14.

Gaillard PJ, Visser CC, de Boer AG (2005). Targeted delivery across the blood–brain barrier. *Expert Opin Drug Deliv* **2**: 299–309.

Gallo JM, Li S, Guo P, Reed K, Ma J (2003). The effect of P-glycoprotein on paclitaxel brain and brain tumor distribution in mice. *Cancer Res* **63**: 5114–5117.

Gelderblom H, Verweij J, van Zomeren DM, Buijs D, Ouwens L, Nooter K *et al.* (2002). Influence of Cremophor El on the bioavailability of intraperitoneal paclitaxel. *Clin Cancer Res* **8**: 1237–1241.

Geney R, Ungureanu M, Li D, Ojima I (2002). Overcoming multidrug resistance in taxane chemotherapy. *Clin Chem Lab Med* **40**: 918–925.

Gupta Jr ML, Bode CJ, Georg GI, Himes RH (2003). Understanding tubulin–Taxol interactions: mutations that impart Taxol binding to yeast tubulin. *Proc Natl Acad Sci USA* **100**: 6394–6397.

Jones AR, Shusta EV (2007). Blood–brain barrier transport of therapeutics via receptor-mediation. *Pharm Res* **24**: 1759–1771.

Kemper EM, Boogerd W, Thuis I, Beijnen JH, van Tellingen O (2004). Modulation of the blood–brain barrier in oncology: therapeutic opportunities for the treatment of brain tumours? *Cancer Treat Rev* **30**: 415–423.

Koziara JM, Lockman PR, Allen DD, Mumper RJ (2004). Paclitaxel nanoparticles for the potential treatment of brain tumors. *J Control Release* **99**: 259–269.

Lidar Z, Mardor Y, Jonas T, Pfeffer R, Faibel M, Nass D *et al.* (2004). Convection-enhanced delivery of paclitaxel for the treatment of recurrent malignant glioma: a phase I/II clinical study. *J Neurosurg* **100**: 472–479.

Lockman PR, Koziara JM, Mumper RJ, Allen DD (2004). Nanoparticle surface charges alter blood–brain barrier integrity and permeability. *J Drug Target* **12**: 635–641.

Louis DN (2006). Molecular pathology of malignant gliomas. *Annu Rev Pathol* **1**: 97–117.

McGrogan BT, Gilmartin B, Carney DN, McCann A (2007). Taxanes, microtubules and chemoresistant breast cancer. *Biochim Biophys Acta* **1785**: 96–132.

Nikanjam M, Gibbs AR, Hunt CA, Budinger TF, Forte TM (2007). Synthetic nano-LDL with paclitaxel oleate as a targeted drug delivery vehicle for glioblastoma multiforme. *J Control Release* **124**: 163–171.

Olivier JC, Fenart L, Chauvet R, Pariat C, Cecchelli R, Couet W (1999). Indirect evidence that drug brain targeting using polysorbate 80-coated polybutylcyanoacrylate nanoparticles is related to toxicity. *Pharm Res* **16**: 1836–1842.

Pardridge WM (2007). Blood–brain barrier delivery. *Drug Discov Today* **12**: 54–61.

Rice A, Liu Y, Michaelis ML, Himes RH, Georg GI, Audus KL (2005). Chemical modification of paclitaxel (Taxol) reduces P-glycoprotein interactions and increases permeation across the blood–brain barrier *in vitro* and *in situ*. *J Med Chem* **48**: 832–838.

Rolland Y, Demeule M, Michaud-Levesque J, Beliveau R (2007). Inhibition of tumor growth by a truncated and soluble form of melanotransferrin. *Exp Cell Res* **313**: 2910–2919.

Rose WC (1992). Taxol: a review of its preclinical *in vivo* antitumor activity. *Anticancer Drugs* **3**: 311–321.

Rousselle C, Clair P, Lefauconnier JM, Kaczorek M, Scherrmann JM, Temsamani J (2000). New advances in the transport of doxorubicin through the blood–brain barrier by a peptide vector-mediated strategy. *Mol Pharmacol* **57**: 679–686.

Schinkel AH, Mol CA, Wagenaar E, van Deemter L, Smit JJ, Borst P (1995). Multidrug resistance and the role of P-glycoprotein knockout mice. *Eur J Cancer* **31A**: 1295–1298.

Tanner PG, Holtmannspotter M, Tonn JC, Goldbrunner R (2007). Effects of drug efflux on convection-enhanced paclitaxel delivery to malignant gliomas: technical note. *Neurosurgery* **61**: E880–E882.

Tseng SH, Bobola MS, Berger MS, Silber JR (1999). Characterization of paclitaxel (Taxol) sensitivity in human glioma- and medulloblastoma-derived cell lines. *Neuro Oncol* **1**: 101–108.

Wang S, Zhelev NZ, Duff S, Fischer PM (2006). Synthesis and biological activity of conjugates between paclitaxel and the cell delivery vector penetratin. *Bioorg Med Chem Lett* **16**: 2628–2631.

Wani MC, Taylor HL, Wall ME, Coggon P, McPhail AT (1971). Plant antitumor agents. VI. The isolation and structure of taxol, a novel antileukemic and antitumor agent from *Taxus brevifolia*. *J Am Chem Soc* **93**: 2325–2327.